Biochem. J. (2009) **422**, 139–149 (Printed in Great Britain) doi:10.1042/BJ20082308

8-Bromo-cyclic inosine diphosphoribose: towards a selective cyclic ADP-ribose agonist

Tanja KIRCHBERGER*, Christelle MOREAU†, Gerd K. WAGNER†[1], Ralf FLIEGERT*, Cornelia C. SIEBRANDS*, Merle NEBEL*, Frederike SCHMID*, Angelika HARNEIT*, Francesca ODOARDI‡, Alexander FLÜGEL‡, Barry V. L. POTTER† and Andreas H. GUSE*[2]

*The Calcium Signalling Group, University Medical Center Hamburg-Eppendorf, Center of Experimental Medicine, Institute of Biochemistry and Molecular Biology I: Cellular Signal Transduction, Martinistrasse 52, D-20246 Hamburg, Germany, †Wolfson Laboratory of Medicinal Chemistry, Department of Pharmacy and Pharmacology, University of Bath, Claverton Down, Bath BA2 7AY, U.K., and ‡Department of Neuroimmunology, Institute for Multiple-Sclerosis-Research, University of Göttingen, Waldweg 33, 37073 Göttingen, Germany

cADPR (cyclic ADP-ribose) is a universal Ca^{2+} mobilizing second messenger. In T-cells cADPR is involved in sustained Ca^{2+} release and also in Ca^{2+} entry. Potential mechanisms for the latter include either capacitative Ca^{2+} entry, secondary to store depletion by cADPR, or direct activation of the non-selective cation channel TRPM2 (transient receptor potential cation channel, subfamily melastatin, member 2). Here we characterize the molecular target of the newly-described membrane-permeant cADPR agonist 8-Br-N^1-cIDPR (8-bromo-cyclic IDP-ribose). 8-Br-N^1-cIDPR evoked Ca^{2+} signalling in the human T-lymphoma cell line Jurkat and in primary rat T-lymphocytes. Ca^{2+} signalling induced by 8-Br-N^1-cIDPR consisted of Ca^{2+} release and Ca^{2+} entry. Whereas Ca^{2+} release was sensitive to both the RyR (ryanodine receptor) blocker RuRed (Ruthenium Red) and the cADPR antagonist 8-Br-cADPR (8-bromo-cyclic ADP-ribose), Ca^{2+} entry was inhibited by the Ca^{2+} entry blockers Gd^{3+} (gadolinium ion) and SKF-96365, as well as by 8-Br-cADPR. To unravel a potential role for TRPM2 in sustained Ca^{2+} entry evoked by 8-Br-N^1-cIDPR, TRPM2 was overexpressed in HEK (human embryonic kidney)-293 cells. However, though activation by H_2O_2 was enhanced dramatically in those cells, Ca^{2+} signalling induced by 8-Br-N^1-cIDPR was almost unaffected. Similarly, direct analysis of TRPM2 currents did not reveal activation or co-activation of TRPM2 by 8-Br-N^1-cIDPR. In summary, the sensitivity to the Ca^{2+} entry blockers Gd^{3+} and SKF-96365 is in favour of the concept of capacitative Ca^{2+} entry, secondary to store depletion by 8-Br-N^1-cIDPR. Taken together, 8-Br-N^1-cIDPR appears to be the first cADPR agonist affecting Ca^{2+} release and secondary Ca^{2+} entry, but without effect on TRPM2.

Key words: Ca^{2+} entry, Ca^{2+} release, cyclic ADP-ribose (cADPR), cyclic ADP-ribose (cADPR) analogue, T-cell activation, transient receptor potential cation channel, subfamily melastatin, member 2 (TRPM2).

INTRODUCTION

cADPR (cyclic ADP-ribose) is a universal Ca^{2+} mobilizing second messenger (reviewed in [1–4]). Receptor-mediated formation has been demonstrated for several cell types and multiple ligands/receptors (reviewed in [1–4]). Formation of cADPR in eukaryotic cells proceeds via ADP-ribosyl cyclases, among which the multifunctional ectoenzyme CD38 is best characterized (reviewed in [5]). Originally, cADPR was discovered as the endogenous nucleotide that releases Ca^{2+} from intracellular stores of sea urchin eggs [6,7]. However, involvement of cADPR in Ca^{2+} entry was discovered approx. ten years later in human T-lymphocytes [8].

Ca^{2+} entry in T-lymphocytes is a process essential for proliferation, as a continuously elevated level of the free cytosolic and nuclear Ca^{2+} concentration ($[Ca^{2+}]_i$) is necessary for continuous activation of the Ca^{2+} and calmodulin-dependent protein phosphatase calcineurin [9]. The latter dephosphorylates NF-AT (nuclear factor of activated T-cells) thereby allowing translocation of NF-AT into the nucleus [10,11].

As a mechanism for Ca^{2+} entry in T-cells, capacitative Ca^{2+} entry [12] has long been postulated (reviewed in [13]). With the discovery of key proteins involved, e.g. Orai1/CRACM1 (calcium release-activated calcium modulator 1) [14,15] and Stim1 (stromal interaction molecule 1) [16], it became clear that Stim1, by sensing decreasing luminal Ca^{2+} concentration upon store depletion, would activate Ca^{2+} entry involving Orai1/CRACM1 as channels, or as part of a larger channel complex. In T-lymphocytes we have demonstrated a crucial role for cADPR in Ca^{2+} entry, as blockade of cADPR action resulted in reduced Ca^{2+} signalling, especially in the sustained phase [17]. Importantly, subsequent signalling events, e.g. CD25 and MHC-II (myosin heavy chain-II) expression, as well as proliferation, were likewise inhibited by cADPR antagonism [17].

Here, we characterize the Ca^{2+} entry mechanism activated by the novel cADPR agonist, 8-Br-N^1-cIDPR (8-bromo-cyclic IDP-ribose) [18]. The advantages of this molecule over natural cADPR are its ability to permeate membranes and its metabolic stability. Indeed, we recently showed that substitution of the amino/imino-group at C^6 by an oxo-group, thus converting the bond between

Abbreviations used: ADPR, ADP-ribose; 8-Br-cADPR, 8-bromo-cyclic ADP-ribose; 8-Br-IDPR, 8-bromo-IDP-ribose; 8-Br-N^1-cIDPR, 8-bromo-cyclic IDP-ribose; 8-Br-NHD, 8-bromo-nicotinamide hypoxanthine dinucleotide; cADPR, cyclic ADP-ribose; DMEM, Dulbecco's modified Eagle's medium; EGFP, enhanced green fluorescent protein; Fura-2AM, Fura-2-acetoxymethyl ester; HEK, human embryonic kidney; IP_3, D-*myo*-inositol-1,4,5-trisphosphate; MBP, myelin basic protein; NAADP, nicotinic acid adenine dinucleotide phosphate; NF-AT, nuclear factor of activated T-cells; Orai1/CRACM1, ORAI calcium release-activated calcium modulator 1; RP-HPLC, reverse-phase HPLC; RuRed, Ruthenium Red; RyR, ryanodine receptor; Stim1, stromal interaction molecule 1; TCA, trichloroacetic acid; TFA, trifluoroacetic acid; TRPM2, transient receptor potential cation channel, subfamily melastatin, member 2.

[1] Current address: School of Chemical Sciences and Pharmacy, University of East Anglia, Norwich NR4 7TJ, U.K.

[2] To whom correspondence should be addressed (email guse@uke.uni-hamburg.de).

N^1 and $C^{1''}$ at the northern ribose into part of a much more chemically stable amide system, produces a compound that is also biologically stable [18].

EXPERIMENTAL

Drugs and materials

8-Br-NHD (8-bromo-nicotinamide hypoxanthine dinucleotide) and cADPR were obtained from Biolog. 8-Br-N^1-cIDPR was either synthesized and purified as described below (see also Figure 1) or obtained from Biolog. ADP-ribosyl cyclase from *Aplysia californica*, 8-Br-cADPR and $GdCl_3$ were from Sigma–Aldrich. RuRed (Ruthenium Red), SKF-96365, TCA (trichloroacetic acid), diethyl ether, methanol (LiChrosolv) and TFA (trifluoroacetic acid) were from Merck Chemicals. Rat anti-CD3 antibody, goat anti-mouse IgM and Lipofectamine™ 2000 were obtained from Invitrogen. Q-Sepharose Fast Flow and G10 Sephadex were obtained from Amersham Bioscience. FuGENE 6 was from Roche Applied Science. All other chemicals used were of the highest purity grade and purchased from Merck Chemicals, Fluka or Sigma–Aldrich. Culture medium reagents were supplied by Sigma–Aldrich, Invitrogen or Biochrom.

Cell culture

Jurkat T-lymphocytes (subclone JMP) were cultured as described previously in [19] at 37 °C in the presence of 5 % CO_2 in RPMI 1640 medium containing Glutamax I and Hepes (25 mM) and supplemented with 7.5 % (v/v) NCS (newborn calf serum), 100 units/ml penicillin and 100 μg/ml streptomycin.

MBP (myelin basic protein)-specific T-cell clones were established from lymph node preparations of pre-immunized Lewis rats. Stimulation, expansion and culture of specific rat T-cells were conducted under conditions described in [20]. For determination of Ca^{2+} signalling, frozen rat T-cells were thawed und cultured in DMEM (Dulbecco's modified Eagle's medium) with Glutamax I, 4.5 g/l glucose, 100 units/ml penicillin, 100 μg/ml streptomycin, 1 mM sodium pyruvate, 10 % (v/v) horse serum, 0.004 % (v/v) 2-mercaptoethanol, 1 % (v/v) non-essential amino acids and 0.04 g/l asparagine at 37 °C in the presence of 10 % CO_2. Resting state T-cells were used in all experiments.

HEK (human embryonic kidney)-293 cells were cultured at 37 °C in the presence of 5 % CO_2 in DMEM medium containing Glutamax I and supplemented with 10 % (v/v) FBS (fetal bovine serum), 100 units/ml penicillin and 100 μg/ml streptomycin.

Synthesis and purification of 8-Br-N^1-cIDPR

8-Br-N^1-cIDPR was synthesized as described previously in [21]. 8-Br-NHD (100 μmol) was incubated with 40 μg *Aplysia californica* ADP-ribosyl cyclase in 25 mM Hepes, pH 7.4, for 15 h at room temperature (24 °C) under continuous stirring in the dark. ADP-ribosyl cyclase was removed by stepwise centrifugation for 1–2 h, at 4000 ***g*** and 4 °C, by use of centrifugal filter devices type Centriprep YM-10 (10 kDa cut-off, Millipore). Synthesis of 8-Br-N^1-cIDPR was confirmed by RP (reverse-phase)-HPLC. Purification was carried out as previously described in [21] or by anion-exchange chromatography and gel filtration to remove the by-products 8-Br-IDPR and nicotinamide. For anion-exchange chromatography, Q-Sepharose Fast Flow was washed four times with water, four times with 500 mM NaCl and five times with purified water. Q-Sepharose Fast Flow (0.5 ml) was packed in plastic filtration tubes (Supelco) and washed with 10 ml of purified water. The aqueous solution of 8-Br-N^1-cIDPR was diluted 5-fold with purified water, to reduce ionic strength, and applied to the column in 3 ml aliquots. The column was washed twice with 5 ml of purified water. Elution of 8-Br-N^1-cIDPR was carried out by subsequent addition of 1.5 ml of NaCl solution at 20, 40, 60, 80, 100, 120, 140, 160, 180, 200 and 250 mM. The eluates were collected and analysed by RP-HPLC. Eluates that contained only 8-Br-N^1-cIDPR (40–100 mM NaCl) were combined. Salt was removed form the purified 8-Br-N^1-cIDPR by gel filtration on Sephadex G10. For gel filtration, 30 g of Sephadex G10 was suspended in 100 ml of water, heated for 1 h at 90 °C and washed 4 times with water. A suspension with 75 % (w/v) Sephadex G10 was prepared, degassed, packed in a glass column (1.5 cm × 30 cm) and compacted for 16 h by gravity flow of water. The solution of 8-Br-N^1-cIDPR was chromatographed with water as eluent. Eluates were collected in a volume of 1–5 ml, analysed by RP-HPLC, combined and freeze-dried. Final characterization of purity and identity was done on RP-HPLC (see Figure 1).

Determination of membrane permeability of 8-Br-N^1-cIDPR

Jurkat T-cells ($\sim 2 \times 10^8$–2.5×10^8) were harvested by centrifugation (550 ***g*** for 5 min at 4 °C), washed once with buffer A (containing 20 mM Hepes, pH 7.4, 140 mM NaCl, 5 mM KCl, 1 mM $MgSO_4$, 1 mM $CaCl_2$, 1 mM NaH_2PO_4 and 5.5 mM glucose), resuspended in 1 ml of buffer A and were kept at room temperature for 10 min. 8-Br-N^1-cIDPR (3 μmol) was added and cells were incubated for 5 min at room temperature, placed on an ice-salt bath for 3 min, harvested by centrifugation (550 ***g***) at 4 °C and washed once with 5 ml of ice cold buffer A. Determination of membrane permeability of 8-Br-N^1-cIDPR was performed in a similar way, as previously described for endogenous ADPR in [22]. Briefly, cells were lysed in TCA, and cell debris was removed. The samples were divided in half, and to one half 50 nmol 8-Br-N^1-cIDPR was added, to identify the 8-Br-N^1-cIDPR peak by HPLC and to calculate the recovery during the extraction. Protein precipitates were removed, and the supernatants were neutralized by extraction with diethyl ether. The samples were then purified by solid-phase extraction. For solid-phase extraction plastic filtration tubes (Supelco) were packed with Q-Sepharose Fast Flow and were cleaned in place with 150 mM TFA. Columns were equilibrated with 10 mM Tris/HCl, pH 8.0. The cellular extracts were diluted with 10 mM Tris/HCl, pH 8.0 and applied to the columns. The columns were washed with 10 mM Tris/HCl, pH 8.0, followed by 600 μl of 40 mM TFA. For the elution of 8-Br-N^1-cIDPR, 1 ml of a 80 mM TFA solution was applied. Samples were neutralized by NaOH, filtered through 0.2 μm filters (Sartorius) and analysed by RP-HPLC as described below. As a control the non-brominated dinucleotide NHD (nicotinamide hypoxanthine dinucleotide) was used in parallel.

RP-HPLC

RP-HPLC analysis of nucleotides was performed on a 250 mm × 4.6 mm Multohyp BDS-C18 5μ column (CS Chromatographie Service) equipped with a 17 mm × 4.6 mm guard column or with a 4.0 mm × 3.0 mm guard cartridge containing a C18 ODS filter element (Phenomenex). The separation was performed as described previously in [23] at a flow rate of 1 ml/min with RP-HPLC buffer (20 mM KH_2PO_4, 5 mM tetrabutylammonium dihydrogen phosphate, pH 6) containing increasing amounts of methanol. The gradient used for separation was usually, 0 min (6.5 % methanol), 3.5 min (7.5 % methanol), 5.5 min (16 % methanol), 8 min (25 % methanol), 18 min

(6.5 % methanol) and 27 min (6.5 % methanol). For separation of 8-Br-N^1-cIDPR in cell extracts the following gradient was used: 0 min (6.5 % methanol), 1.5 min (6.5 % methanol), 3.5 min (7.5 % methanol), 5.5 min (16 % methanol), 6.5 min (16 % methanol), 14 min (32.5 % methanol), 16 min (32.5 % methanol), 18 min (6.5 % methanol) and 27 min (6.5 % methanol). Nucleotides were detected using an UV detector (HPLC detector 432, Kontron Instruments) or a DAD (photo diode array detector 1200 series, Agilent Technologies) at 250 nm and 260 nm for hypoxanthine or at 270 nm for adenine-based nucleotides respectively. Integration of peaks was performed with the data-acquisition system MT2 from Kontron Instruments or with the Rev. B.02.01 ChemStation from Agilent technologies. Quantification was performed with external standards.

Transient transfection of HEK-293 cells

A cDNA containing the total ORF (open reading frame) of human TRPM2 (transient receptor potential cation channel, subfamily melastatin, member 2) was amplified from human RNA by one-step RT (reverse transcription)–PCR using the Titan One-Tube RT-PCR kit (Roche) according to the manufacturer's instructions (forward primer including EcoRI site, 5′-GGAATTCATGGAGCCCTCAGCCCTG-3′; reverse primer including a SalI site, 5′-TACTGTCGACTCAGTAGTGAGCCCC-3′). The resulting amplicon was cloned into the EcoRI and SalI sites of the multiple cloning site of pIRES2-EGFP (enhanced green fluorescent protein) (Clontech). This vector was termed pIRES2-EGFP-TRPM2.

For transfection, HEK-293 cells were seeded in 35 mm dishes, cultured to a density of 50–80 % of confluency and were transfected by addition of transfection mixture consisting of 100 μl of OptiMEM, 3 μl of FuGENE or 3 μl of Lipofectamine™ 2000 and 1 μg of plasmid DNA (pIRES2-EGFP or pIRES2-EGFP-TRPM2) to the cells. For transfection with FuGENE, transfection mixture was added directly to the cell culture medium, whereas transfection with Lipofectamine™ 2000 was carried out in OptiMEM. For Ca^{2+}-imaging experiments, transfected cells were seeded in 8-well slides (ibidi) coated with poly-L-lysine (70–150 kDa) at a low cell density.

Ratiometric Ca^{2+} imaging

Jurkat T-cells were loaded with Fura-2AM (Fura-2-acetoxymethyl ester) as described in [19] and kept in the dark at room temperature until use. Primary rat T-cells were loaded with 12 μM Fura-2AM and 2 mM probenicid for 30 min at 37 °C in the dark, washed twice with buffer A and kept in the dark at 15–18 °C until use. HEK-293 cells were loaded in 8-well slides with 4 μM Fura-2AM in HEK-293 cell medium for 30 min at 37 °C in the dark and washed twice with buffer A.

For Ca^{2+} imaging of Jurkat T-cells or rat T-cells thin glass coverslips (0.1 mm) were coated first with BSA (5 mg/ml) and subsequently with poly-L-lysine (0.06–0.1 mg/ml). Silicon grease was used to seal small chamber slides, consisting of a rubber O-ring, on the glass coverslip. Then, 40–60 μl of buffer A and 40 μl of T-cell suspension ($\sim 1 \times 10^6$–2×10^6 cells/ml) in the same buffer were added into the small chamber. Where the calcium free/calcium re-addition protocol was used, 0.2×10^6 Jurkat T-cells were washed twice in nominal Ca^{2+}-free buffer A and added to the small chamber. The time the cells were held under Ca^{2+}-free conditions was kept as short as possible to avoid emptying of the ER (endoplasmic reticulum) Ca^{2+} pool; such emptying due to prolonged exposure to Ca^{2+} free conditions resulted in very low or undetectable Ca^{2+} signals upon cADPR microinjections in a previous study [8]. The loaded coverslip or 8-well slide was mounted on the stage of a Leica DMIRE2 fluorescence microscope. In some experiments Jurkat T-cells were preincubated with $GdCl_3$ (25 μM), SKF-96365 (30 μM) or 8-Br-cADPR (500 μM) in buffer A. In experiments with $GdCl_3$, Na_2HPO_4 was not included in buffer A, to prevent precipitation of $GdPO_4$.

Ratiometric Ca^{2+} imaging was performed as described in [24]. We used an Improvision imaging system, built around the Leica microscope, at 40- or 100-times magnification. Illumination at 340 and 380 nm was carried out using a monochromator system (Polychrom IV, TILL Photonics). Images were taken with a gray-scale charge-coupled device camera (type C 4742–95–12ER; Hamamatsu) operated in 8-bit mode. The spatial resolution was 512×640 pixels. Camera exposure times were 12–30 ms (at 340 nm) and 4–10 ms (at 380 nm) at a 3:1 ratio. The acquisition rate was adjusted to $\sim$14 ratios per minute. Raw data images were stored on a hard disk and ratio images (340/380 nm) were constructed pixel by pixel. Confocal Ca^{2+} images were obtained by off-line deconvolution using the volume deconvolution module and a no-neighbour algorithm in the Openlab software (Improvision) as described recently for 3T3 fibroblasts in [25]. The deconvoluted images were used to construct ratio images (340/380 nm) pixel by pixel. Finally, ratio values were converted into Ca^{2+} concentrations by external calibration as described in [24]. Data processing was performed using Openlab software, version 3.0.8 or 1.7.8.

Microinjection

Microinjections were carried out as described in [8]. We used an Eppendorf system (transjector type 5171, micromanipulator type 5246) or Femtojet (Eppendorf AG) with Femtotips I or II as pipettes. 8-Br-N^1-cIDPR or cADPR were diluted to their final concentration in intracellular buffer (20 mM Hepes, pH 7.2, 110 mM KCl, 10 mM NaCl), filtered (0.2 μm) and centrifuged (15 700 ***g*** for 10 min at 4 °C) before use. Injections were made using the semiautomatic mode of the system with the following instrumental settings: injection pressure 6–8 kPa, compensatory pressure 2.5–4 kPa, injection time 0.5 s and velocity of the pipette 700 μm/s.

Electrophysiology

Membrane currents were recorded in the whole cell configuration of the patch clamp technique as described in [26]. An EPC10 USB patch clamp amplifier was used in conjunction with the PULSE stimulation and data acquisition software (HEKA Elektronik). Data were sampled at 5 kHz and compensated for both fast and slow capacity transients. Series resistance was compensated by 70 %. All experiments were performed at room temperature with Jurkat T-cells attached to tissue culture dishes before the experiment. The pipette solution contained 10 mM Hepes, pH 7.2 (adjusted with KOH), 140 mM KCl, 1 mM $MgCl_2$ and 8 mM NaCl. In some experiments, the pipette solution additionally contained ADPR (30, 100, 300 or 1000 μM), cADPR (30, 100, 300 or 1000 μM), 8-Br-N^1-cIDPR (300 μM), ADPR (30 μM) plus either cADPR (5 μM or 100 μM) or 8-Br-N^1-cIDPR (300 μM). The external solution contained 10 mM Hepes, pH 7.4 (adjusted with NaOH), 140 mM NaCl, 2 mM $MgCl_2$, 2 mM $CaCl_2$, 5 mM KCl and 5 mM glucose. The cells were held at -60 mV and current–voltage relations were obtained every 5 s using 250 ms voltage ramps from -85 to -65 mV.

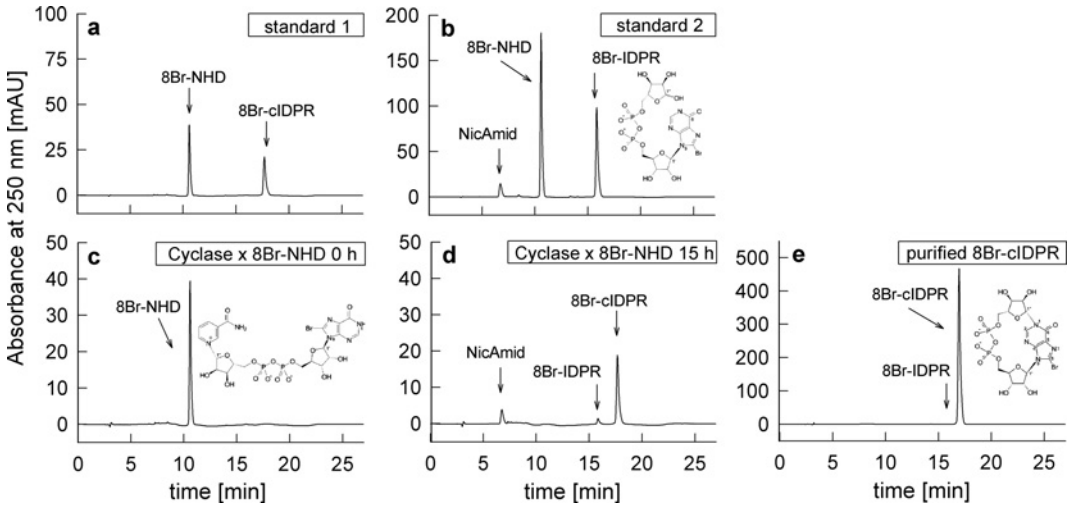

Figure 1 Synthesis of 8-Br-N^1-cIDPR

(**a**) RP-HPLC of standard 1, 8-Br-NHD and 8-Br-N^1-cIDPR (8-Br-cIDPR). (**b**) RP-HPLC of standard 2, nicotinamide (NicAmid), 8-Br-NHD and 8-Br-IDPR. 8-Br-IDPR was synthesized by incubation of 8-Br-NHD with NADase of *Neurospora crassa*. 1 mM 8-Br-NHD was incubated with 1 μg/μl ADP-ribosyl cyclase of *A. californica* in 25 mM Hepes, pH 7.4, for 15 h at room temperature. Aliquots were taken at (**c**) 0 h and (**d**) 15 h and analysed by RP-HPLC. (**e**) RP-HPLC of purified 8-Br-N^1-cIDPR.

RESULTS

8-Br-N^1-cIDPR was prepared by quantitative conversion of 8-Br-NHD into 8-Br-N^1-cIDPR using *A. californica* ADP-ribosyl cyclase (Figure 1). Comparison of the products after a 15 h incubation period with standards clearly showed that the main product was 8-Br-N^1-cIDPR. However, a small portion of 8-Br-NHD was converted into the linear product 8-Br-IDPR (Figure 1d). This small contamination of 8-Br-IDPR was quantitatively removed by anion-exchange chromatography using Sepharose Q Fast Flow followed by desalting of purified 8-Br-N^1-cIDPR on Sephadex 10 Fast Flow. The final product showed a purity of almost 100 % on HPLC (Figure 1e).

Although we had reported previously [21] that 8-Br-N^1-cIDPR is membrane-permeant we initially assessed the biological activity of 8-Br-N^1-cIDPR in combined microinjection and Ca^{2+} imaging experiments. This was in order to obtain a proper concentration–response relationship without any potential additional effects, due to membrane permeancy and/or pumping out of the compound by multiple drug resistance transporters. Whereas microinjection of intracellular buffer into intact Fura-2AM-loaded Jurkat T-cells had little effect (Figure 2a), the natural cADPR showed a robust response when microinjected at 100 μM (Figure 2b). It must be noted here that in such microinjection experiments only $\sim$1–1.5 % of the cell volume is injected [8], resulting in an effective intracellular concentration far below the pipette concentration. At 100 μM, 8-Br-N^1-cIDPR evoked Ca^{2+} signalling only in some cells (Figure 2c), whereas at pipette concentrations of $\geqslant$1 mM 8-Br-N^1-cIDPR, robust Ca^{2+} responses were recorded, consisting of a rapid and high Ca^{2+} peak within tens of seconds followed by a lower, but sustained plateau phase (Figure 2d–2f). The effect was saturable and showed an EC_{50} of about 300 μM (Figure 2g).

Importantly, the 8-substitution with bromine in 8-Br-N^1-cIDPR resulted in a membrane-permeant molecule, as already determined in initial experiments [21]. To check the membrane permeabilty of 8-Br-N^1-cIDPR directly, Jurkat T-cells were incubated with 8-Br-N^1-cIDPR for 5 min, then cellular nucleotides were extracted with TCA and crude cell extracts were purified by solid-phase extraction and analysed by RP-HPLC (Figure 3) in a similar way as described for ADPR in

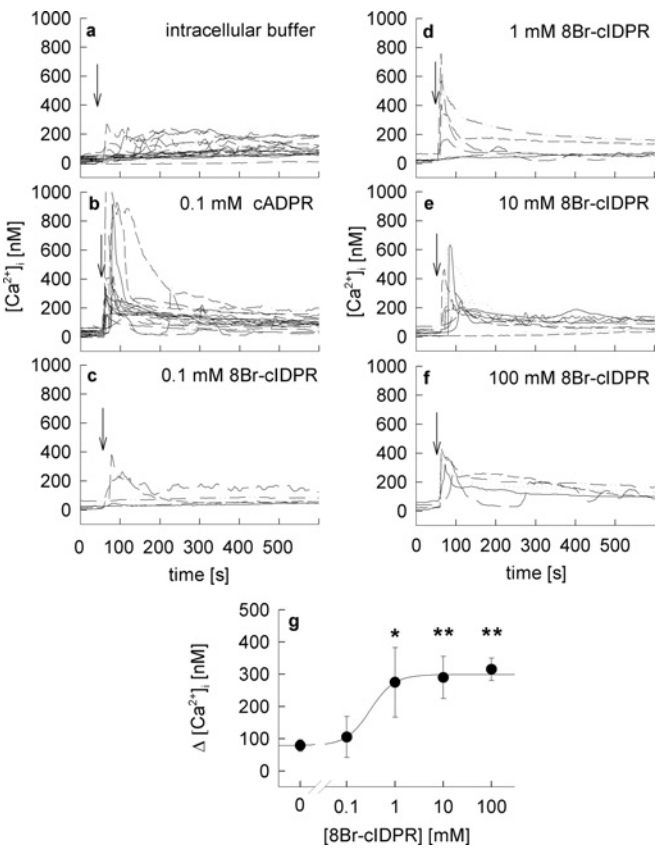

Figure 2 Microinjection of 8-Br-N^1-cIDPR in intact Jurkat T-cells

Jurkat T-cells were loaded with Fura-2AM and subjected to combined Ca^{2+} imaging and microinjection. Time points of microinjection are indicated by arrows. Cells were microinjected (**a**) with intracellular buffer (n = 21) or (**b**) or 100 μM cADPR, (n = 20) as controls or with (**c**) 0.1 mM (n = 6), (**d**) 1 mM (n = 7), (**e**) 10 mM (n = 10) or (**f**) 100 mM (n = 5) 8-Br-N^1-cIDPR. (**g**) Concentration–response curve of 8-Br-N^1-cIDPR. Results are shown as means $\pm$ S.E.M. (n = 5–21) of single tracings from time points 50–100 s (the Ca^{2+} peak). *, $P < 0.01$; **, $P < 0.001$ (t test).

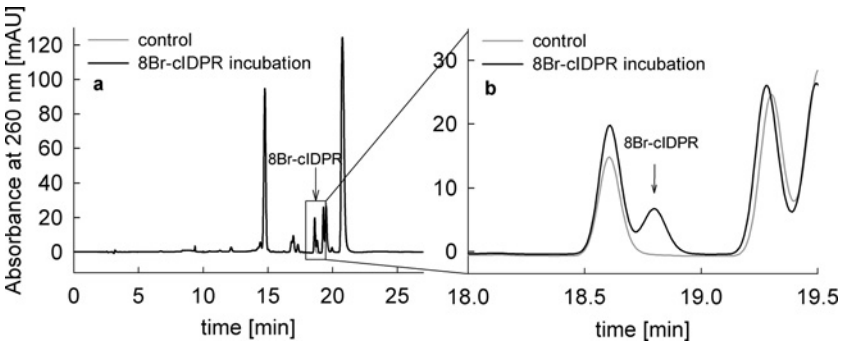

Figure 3 Membrane permeability of 8-Br-N^1-cIDPR

Jurkat T-cells were incubated with 3 mM 8-Br-N^1-cIDPR for 5 min at room temperature. Cellular nucleotides were extracted with TCA. Crude cell extracts were purified by solid-phase extraction and analysed by RP-HPLC. (**a**) Representative RP-HPLC analysis of absorbed 8-Br-N^1-cIDPR in Jurkat T-cells is shown (black line). (**b**) Magnification of the trace shown in (**a**). The peak of 8-Br-N^1-cIDPR is indicated by an arrow. As a control, cell extracts of cells not incubated with 8-Br-N^1-cIDPR were analysed by HPLC (grey line). Jurkat T-cells incubated with 8-Br-N^1-cIDPR took up 0.16 fmol per cell with a recovery of about 88 %. Results are means ($n = 2$).

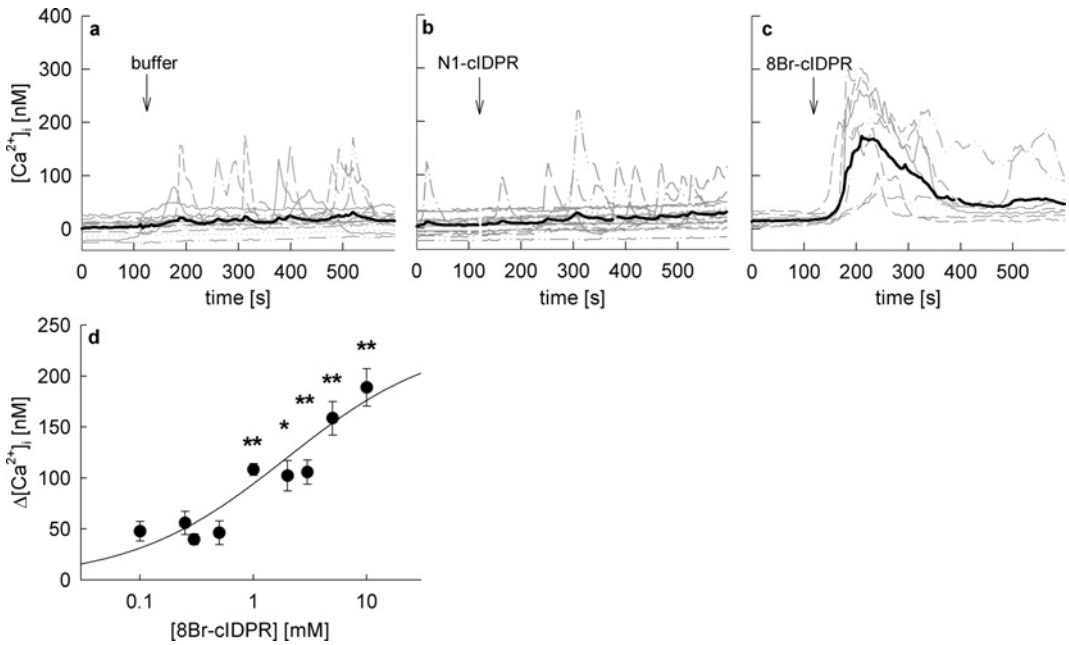

Figure 4 Extracellular addition of 8-Br-N^1-cIDPR evoked Ca^{2+} signalling in intact Jurkat T-cells

Jurkat T-cells were loaded with Fura-2AM and subjected to Ca^{2+} imaging. The time points of addition of (**a**) buffer, (**b**) 1 mM *N*1-cIDPR and (**c**) 1 mM 8-Br-N^1-cIDPR are indicated by arrows. Characteristic tracings from a representative experiment are shown. (**d**) Concentration–response curve of 8-Br-N^1-cIDPR. Results represent means ± S.E.M. ($n = 21–109$) of single tracings from time points 100–400 s (of the 8-Br-N^1-cIDPR mediated Ca^{2+} peak). $^*P < 0.01$ and $^{**}P < 0.001$.

[22]. In Jurkat T-cells incubated with 8-Br-N^1-cIDPR a cellular uptake of 0.16 fmol/cell was measured (Figure 3). In contrast, cells incubated with the non-brominated dinucleotide NHD did not take up this molecule, indicating that bromination is a prerequisite for membrane permeancy (results not shown). In separate experiments, we checked that NHD was not metabolized in the time period of the uptake experiments.

Addition of membrane permeant 8-Br-N^1-cIDPR to intact Jurkat T-cells induced a dose-dependent Ca^{2+} signal (Figure 4). At concentrations $\geqslant$1 mM, 8-Br-N^1-cIDPR induced a rapid Ca^{2+} response in these cells consisting of a Ca^{2+} peak and a small but sustained plateau phase (Figure 4c), whereas no Ca^{2+} signal was mediated by addition of the non-brominated analogue N^1-cIDPR (Figure 4b) or buffer (Figure 4a). As 8-Br-N^1-cIDPR at 1 mM induced robust and significant Ca^{2+} signalling, this extracellular concentration was chosen for most further experiments.

To also test the effect of 8-Br-N^1-cIDPR on primary T-cells, rat MBP-specific T-cells were loaded with Fura-2AM and subjected to Ca^{2+} imaging (Figure 5). Buffer was added as a negative control and cells were stimulated via the T-cell receptor/CD3 complex (using anti-CD3 antibody, followed by cross-linking IgM) as a positive control (Figures 5a and 5b). Although anti-CD3 antibody alone resulted in a robust Ca^{2+} signal, cross-linking of the primary antibody on the surface of the cells further enhanced the stimulation (Figure 5b). Addition of 8-Br-N^1-cIDPR resulted in Ca^{2+} signals with different kinetics and amplitudes with regard to individual cells (Figure 5c). When stimulation with 8-Br-N^1-cIDPR was compared with T-cell receptor/CD3 stimulation, similar individual differences in kinetics were observed (compare Figures 5b and 5c), but peak amplitudes were significantly lower for 8-Br-N^1-cIDPR (Figure 5d). This difference is not unexpected, as in the first

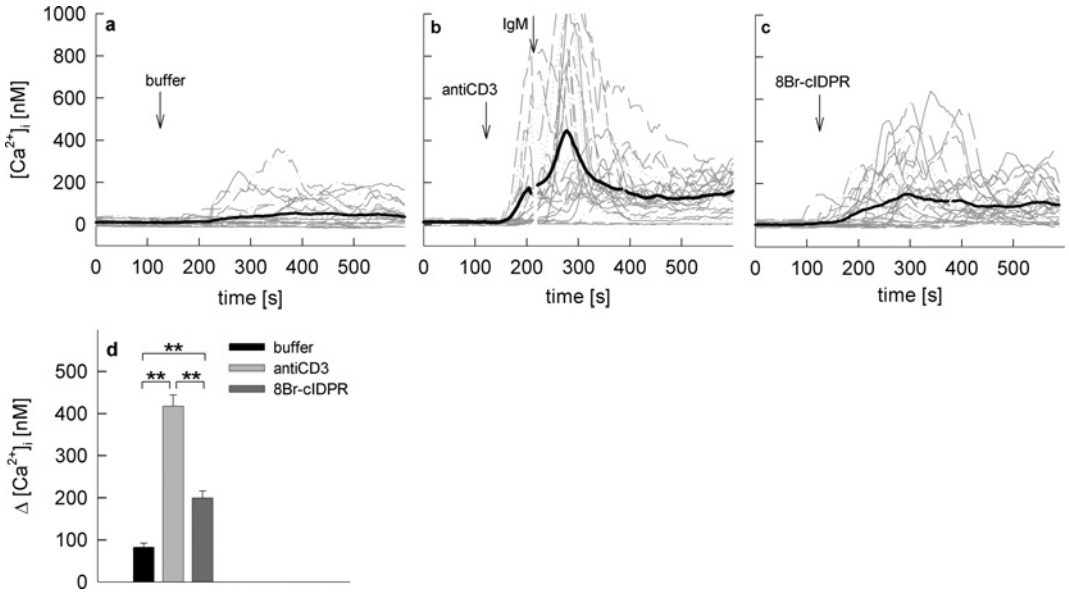

Figure 5 Extracellular addition of 8-Br-N^1-cIDPR evoked Ca^{2+} signalling in primary rat T-cells

Rat T-cells were loaded with Fura-2AM and subjected to Ca^{2+} imaging. The time points of addition of (**a**) buffer, (**b**) anti-CD3 followed by a cross-linking IgM (40 μg/ml and 10 μg/ml) and (**c**) 1 mM 8-Br-N^1-cIDPR are indicated by arrows. Characteristic tracings from a representative experiment are shown. (**d**) Combined results representing means $\pm$ S.E.M ($n = 186–241$) of single tracings from time points 100–400 s (the Ca^{2+} peak). **, $P < 0.001$ (t test).

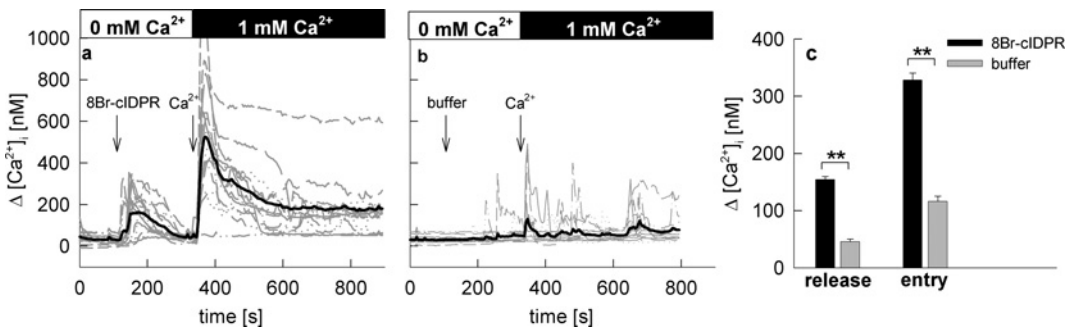

Figure 6 8-Br-N^1-cIDPR activated both Ca^{2+} release and Ca^{2+} entry in intact Jurkat T-cells

Jurkat T-cells were loaded with Fura-2AM and subjected to Ca^{2+} imaging. (**a**) Cells were kept in a nominally Ca^{2+} free buffer in the first part of experiment and 8-Br-N^1-cIDPR was added as indicated. Then, $CaCl_2$ was re-added. (**b**) Buffer was added instead of 8-Br-N^1-cIDPR as a control. The time points of addition of buffer, 1 mM 8-Br-N^1-cIDPR or 1 mM Ca^{2+} are indicated by arrows. Characteristic tracings from representative experiments are shown. (**c**) Combined data representing means $\pm$ S.E.M. ($n = 362–404$) of single tracings from time points 100–200 s (8-Br-N^1-cIDPR mediated Ca^{2+} release-peak) or 300–450 s (8-Br-N^1-cIDPR mediated Ca^{2+} entry-peak). **, $P < 0.001$ (t test).

10 min of T-cell activation at least three Ca^{2+} release systems, NAADP (nicotinic acid adenine dinucleotide phosphate), IP_3 (D-*myo*-inositol-1,4,5-trisphosphate) and cADPR are involved (reviewed in [3,27]). However, 8-Br-N^1-cIDPR mimicked the second phase of T-cell receptor/CD3-mediated Ca^{2+} signalling, once again underpinning the essential role of cADPR in sustained Ca^{2+} signalling in T-cells.

cADPR has been shown not only to act on intracellular Ca^{2+} release via RyR (ryanodine receptor) [17], but also to sensitize the TRPM2 cation channel for its ligand ADPR [28,29]. To analyse the mechanism of the cADPR analogue 8-Br-N^1-cIDPR in more detail, a Ca^{2+}-free–Ca^{2+} reintroduction protocol was used to separate potential Ca^{2+} release and Ca^{2+} entry evoked by 8-Br-N^1-cIDPR (Figure 6). Under Ca^{2+}-free conditions, a robust Ca^{2+} release upon addition of 8-Br-N^1-cIDPR was observed (Figures 6a and 6b). Re-addition of extracellular Ca^{2+} resulted in a huge Ca^{2+} entry overshoot followed by a small sustained plateau phase (Figures 6a and 6b). These results suggest that 8-Br-N^1-cIDPR activates both Ca^{2+} release and Ca^{2+} entry.

Secondly, co-microinjections of 8-Br-N^1-cIDPR with RuRed were carried out (Figure 7). RuRed largely reduced the initial Ca^{2+} peak (Figures 7c and 7d) indicating that this initial peak mainly depends on RyR.

Taken together, we showed that 8-Br-N^1-cIDPR behaved similarly to cADPR. In the next sets of experiments we aimed to analyse in more detail the Ca^{2+} entry pathway activated by 8-Br-N^1-cIDPR by using inhibitors of Ca^{2+} entry, $GdCl_3$ and SKF-96365 [8,30,31]. In both cases robust Ca^{2+} release was observed under Ca^{2+}-free conditions, whereas Ca^{2+} entry was inhibited (Figures 8c, 8d, 8g and 8h). Interestingly, preincubation with Gd^{3+} increased Ca^{2+} release induced by 8-Br-N^1-cIDPR significantly (Figure 8d). A potential explanation for this effect

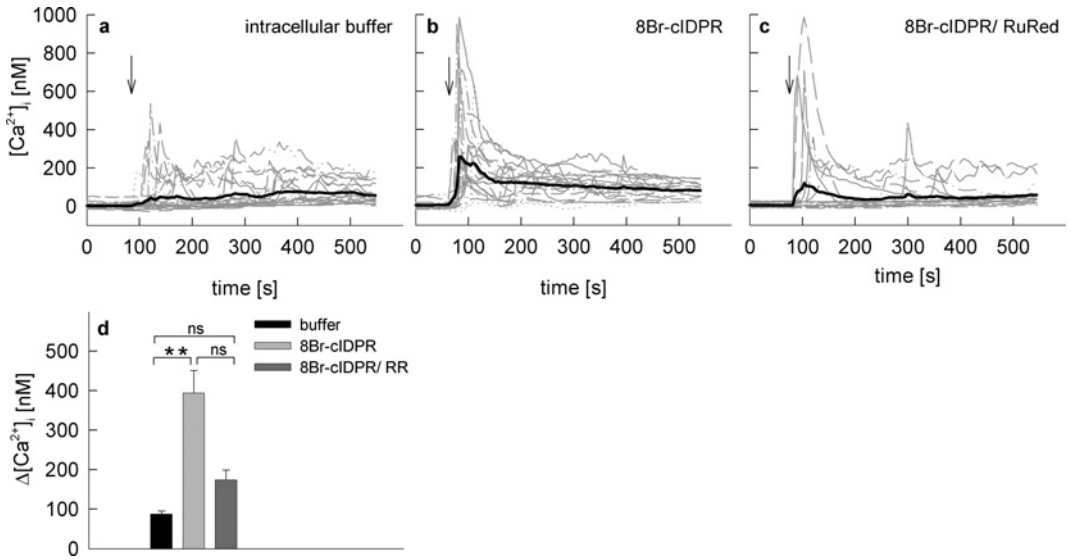

Figure 7 Effect of RuRed on 8-Br-N^1-cIDPR mediated Ca^{2+} signalling in intact Jurkat T-cells

Jurkat T-cells were loaded with Fura-2AM and subjected to combined Ca^{2+} imaging and microinjections. Time points of microinjection are indicated by arrows. Cells were microinjected with (**a**) intracellular buffer ($n = 26$), (**b**) 1 mM 8-Br-N^1-cIDPR ($n = 21$) or (**c**) a mixture of 10 μM RuRed and 1 mM 8-Br-N^1-cIDPR ($n = 20$). (**d**) Combined results representing means $\pm$ S.E.M. of single tracings from time points 50–150 s (the Ca^{2+} peak). **, $P < 0.001$ (t test). ns, not significant.

is the sensitivity of the plasma membrane Ca^{2+}-ATPase to Gd^{3+} [32]; inhibition of Ca^{2+} extrusion in the absence of extracellular Ca^{2+} would in fact result in an apparent increase in $[Ca^{2+}]_i$.

In the presence of the cADPR antagonist 8-Br-cADPR, Ca^{2+} release was partially, but not significantly inhibited (Figures 8k and 8l). Interestingly, there was full inhibition of Ca^{2+} entry under such conditions. It is probable that the incomplete inhibition of Ca^{2+} release is due to the partial antagonist character of 8-Br-cADPR [33]. As discussed above for Ca^{2+} entry, at least two mechanisms may be involved, either the diminished Ca^{2+} release resulted in inhibition of capacitative Ca^{2+} entry via Orai1/CRACM1 channels [34], or direct activation of Ca^{2+} entry by 8-Br-N^1-cIDPR was inhibited by 8-Br-cADPR. As Kolisek et al. [28] previously showed that cADPR, together with ADPR, activates the unspecific cation channel TRPM2, we used HEK-293 cells transiently overexpressing TRPM2 or EGFP (as a negative control) for further experiments. As positive control, Ca^{2+} signalling induced by H_2O_2 was used, as it was previously shown that H_2O_2 increased the open probability TRPM2 [28,35]. These results were confirmed in experiments for the present study (Figures 9a and 9d). In contrast, statistically significant effects between TRPM2-overexpressing cells and controls were not obtained when 8-Br-N^1-cIDPR was used as activator of Ca^{2+} signalling up to extracellular concentrations of 10 mM (Figures 9b, 9e and 9g).

In the next series of experiments direct activation of endogenously expressed TRPM2 in Jurkat T-cells was analysed by patch-clamp recordings in the whole-cell configuration. Infusion of ADPR (300 μM) at a membrane potential of -80 mV evoked a marked inward current (Figure 10a) characterized by an almost linear *IV*-relationship (Figure 10b) and a saturable concentration–response relationship with an EC_{50} of 133 μM (Figure 10c). Infusion of cADPR alone did not activate the TRPM2 current, except for a minor effect at 1 mM cADPR pipette concentration (Figure 10c). However, due to the small contamination of 4 % ADPR (Figure 10e), amounting to 40 μM ADPR, in the pipette, it is probable that ADPR contamination, and not the cADPR in the pipette, induced the current. Comparing the amplitudes evoked by 30 μM ADPR and 1 mM cADPR (containing 40 μM ADPR) further substantiates this conclusion (Figure 10c). Infusion of a combination of a low concentration of ADPR (30 μM) plus cADPR had a small modulatory effect when 100 μM cADPR was used (Figure 10d), indicating a co-modulatory role of cADPR on TRPM2, activated by low concentrations of ADPR, as described in [35]. However, 8-Br-N^1-cIDPR neither activated TRPM2 alone (Figure 10c) nor in combination with low ADPR (Figure 10d).

DISCUSSION

In this report we demonstrate that the membrane-permeant cADPR agonist 8-Br-N^1-cIDPR evokes Ca^{2+} signalling in both the T-lymphoma cell line Jurkat and in primary T-cells. Ca^{2+} signalling induced by 8-Br-N^1-cIDPR consisted of both Ca^{2+} release and Ca^{2+} entry. Whereas Ca^{2+} release was sensitive to both the RyR blocker RuRed and the cADPR antagonist 8-Br-cADPR, Ca^{2+} entry was inhibited by the non-specific Ca^{2+} entry blockers Gd^{3+} and SKF-96365, as well as by 8-Br-cADPR [10]. Activation of TRPM2 by 8-Br-N^1-cIDPR was neither observed in heterologously expressed TRPM2 in HEK-293 cells activated by H_2O_2, nor in endogenously expressed TRPM2 in Jurkat T-cells. Furthermore, 8-Br-N^1-cIDPR did not co-activate TRPM2 when infused together with a low concentration of ADPR.

Stimulation of T-cell Ca^{2+} signalling via the T-cell receptor/CD3 complex involves the subsequent formation of at least three second messengers. Within a few seconds NAADP is produced, peaking after around 10–20 s and returning to the baseline level rapidly [36]. NAADP serves as the initial Ca^{2+} trigger to 'ignite' the Ca^{2+} signalling system of T-cells (for review see [37]). Next, IP_3 is produced transiently, and initiates global Ca^{2+} signalling within the first 15–20 min of T-cell activation [38]. In contrast, cADPR is formed more slowly and continues to release Ca^{2+} from internal stores as IP_3 levels fall [17]. Thus sustained and elevated cADPR levels and sustained Ca^{2+} signalling by cADPR are essential components of T-cell activation

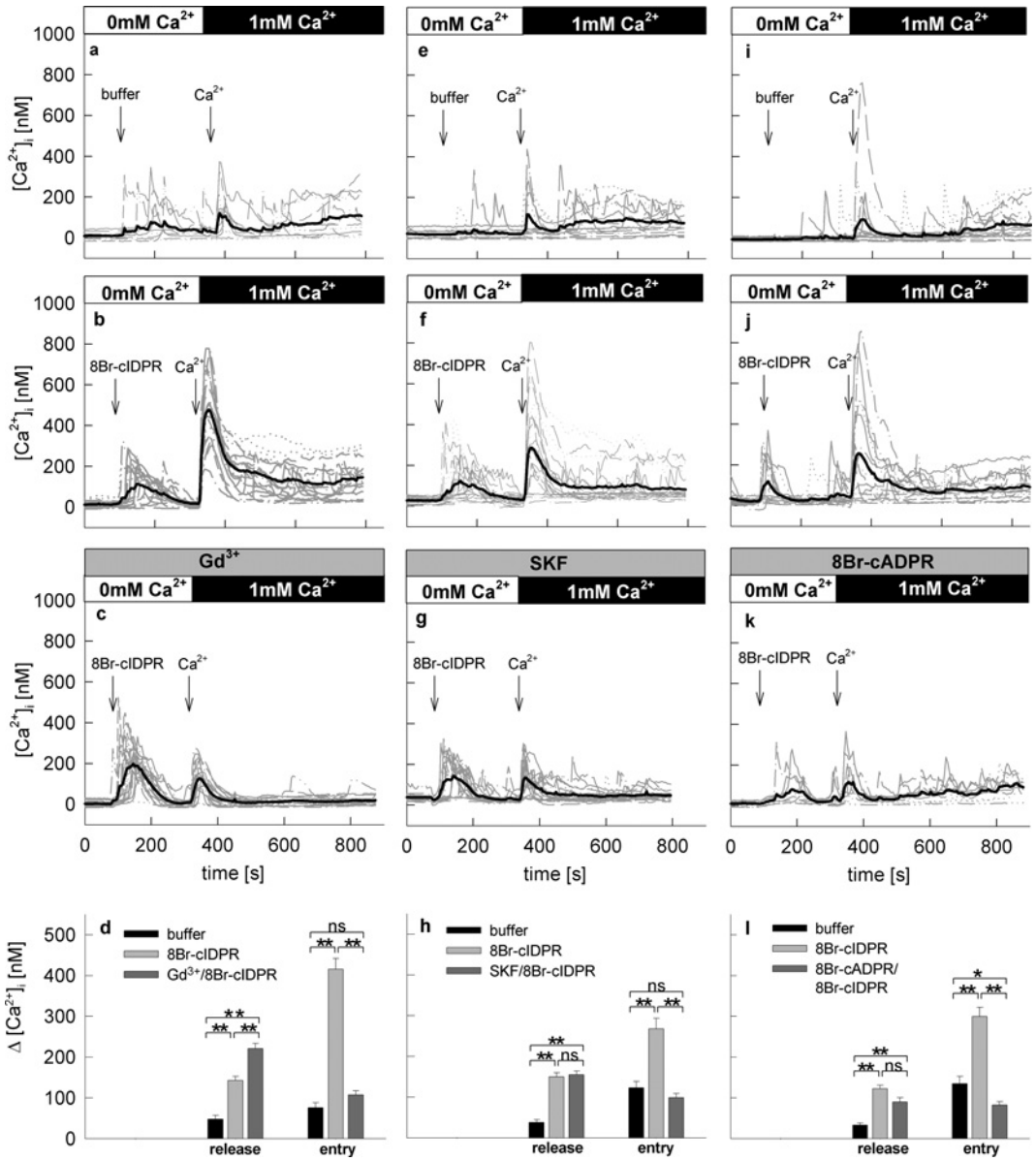

Figure 8 Effect of Gd^{3+}, SKF-96365 and 8-Br-cADPR on Ca^{2+} release and Ca^{2+} entry mediated by 8-Br-N^1-cIDPR in intact Jurkat T-cells

Jurkat T-cells were loaded with Fura-2 and subjected to Ca^{2+} imaging. (**a**), (**e**) and (**i**) show negative controls. Cells were kept in a nominal Ca^{2+} free buffer in the first part of the experiment and buffer was added as indicated and then $CaCl_2$ was re-added. (**b**) (**f**) and (**j**) show positive controls. 8-Br-N^1-cIDPR was added instead of buffer. Cells were preincubated with (**c**) 10 μM Gd^{3+}, (**g**) 30 μM SKF-96365 or (**k**) 500 μM 8-Br-cADPR. Time points of addition of buffer, 1 mM 8-Br-N^1-cIDPR or 1 mM Ca^{2+} are indicated by arrows. Characteristic tracings from a representative experiment are shown. (**d**), (**h**) and (**i**) Combined data representing means $\pm$ S.E.M. ($n = 86–138$) of single tracings from time points 100–200 s (8-Br-N^1-cIDPR mediated Ca^{2+} release-peak), 300–450 s (8-Br-N^1-cIDPR mediated Ca^{2+} entry-peak). *, $P < 0.01$; **, $P < 0.001$ (*t* test).

[17]. As the intracellular Ca^{2+} stores of T-cells are low in capacity, sustained Ca^{2+} signalling is only possible by recruitment of Ca^{2+} entry. In theory, at least two mechanisms for Ca^{2+} entry evoked by the sustained high cADPR levels are possible: either capacitative Ca^{2+} entry [12] via Orai1/CRACM1 channels [14,15] is activated by reduced store loading secondary to cADPR action, or cADPR acts as a co-activator of TRPM2 as described previously [28,29].

As described for a number of membrane-permeant cADPR agonists {e.g. N^1-ethoxymethyl-cIDPR [39], N^1-[(phosphoryl-*O*-ethoxy)-methyl]-N^9-[(phosphoryl-*O*-ethoxy)-methyl]-hypoxanthine-cyclic pyrophosphate [40], 2′,3′-dideoxy-didehydro-cyclic ADP-carbocyclic ribose [41], 8-phenyl-cIDPR [42] and N^1-[(5′-*O*-phosphoryl)ethoxyethyl]-5-*O*-phosphoryladenosine 5′,5′-cyclic pyrophosphate [43]} 8-Br-N^1-cIDPR essentially mimicks the cADPR branch of T-cell Ca^{2+} signalling. However, for none of these cADPR agonist analogues has the mechanism of Ca^{2+} entry been elucidated. As 8-Br-NHD, the synthetic precursor of 8-Br-N^1-cIDPR, can be easily synthesized in large quantities, and since 8-Br-N^1-cIDPR can then be formed in high yield chemo-enzymatically [21], we performed this detailed analysis of cADPR-mediated Ca^{2+} entry using 8-Br-N^1-cIDPR as a cADPR agonist. The advantage of this strategy is the precise activation of only the cADPR/RyR branch, whereas the disadvantage is that any signalling cross-talk from other pathways triggered upon T-cell activation that may modulate the cADPR/RyR branch is not involved.

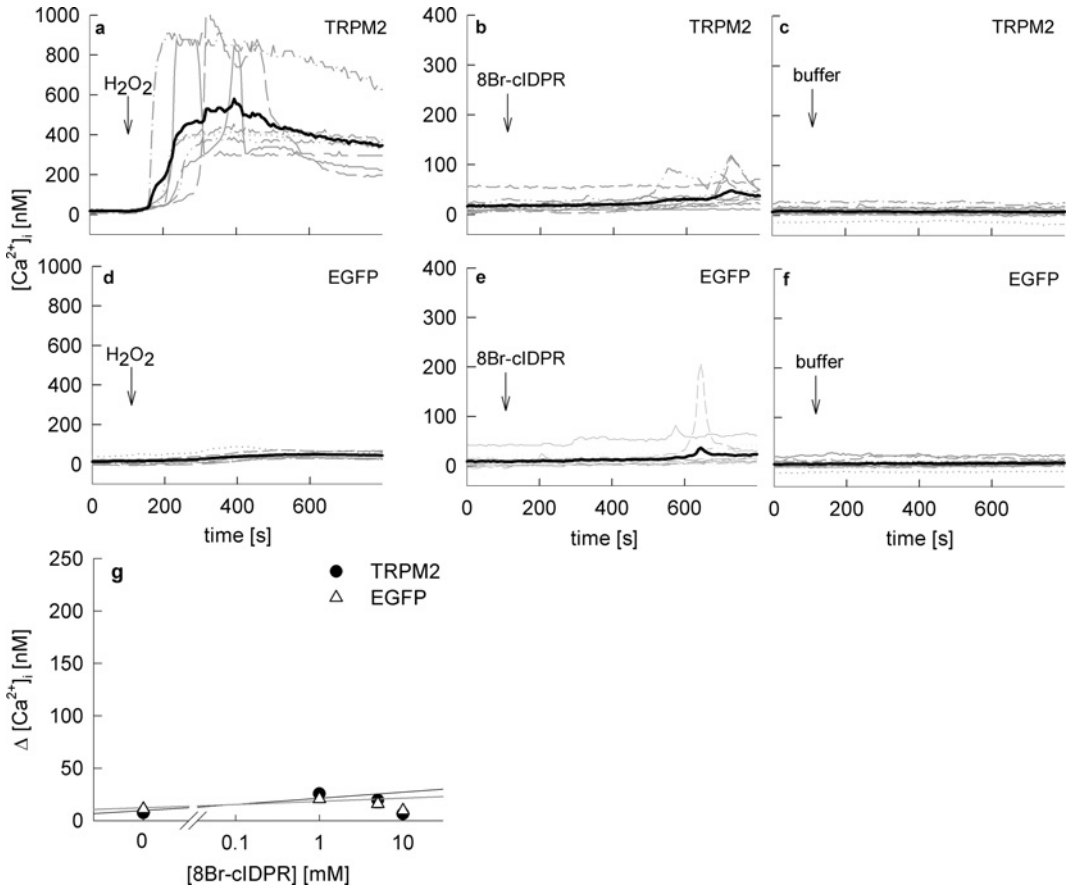

Figure 9 Effect of 8-Br-N^1-cIDPR on Ca^{2+} signalling in HEK293 cells overexpressing TRPM2

HEK-293 cells transfected with (**a**)–(**c**) pIRES2-EGFP-TRPM2 (TRPM2) and (**d**)–(**f**) pIRES2-EGFP (EGFP control) were loaded with Fura-2AM and subjected to Ca^{2+} imaging. Time points of addition of a maximal concentration of (**a** and **d**) 100 or 300 μM H_2O_2, (**b**) and (**e**) 1 mM 8-Br-N^1-cIDPR, or (**c**) and (**f**) buffer are indicated. Characteristic tracings of a representative experiment are shown. (**g**) Concentration–response curve of 8-Br-N^1-cIDPR in transfected HEK-293 cells ($n = 6$–67) represented as means $\pm$ S.E.M. of single tracings from time points 100–600 s (the Ca^{2+} peak).

TRPM2 channel opening was described to be regulated by ADPR, with cADPR also playing a crucial role as co-activator [28,29]. Furthermore, co-activator effects of cADPR towards TRPM2 are sensitive to the cADPR antagonist 8-Br-cADPR [35]. Since we observed that 8-Br-cADPR effectively inhibits Ca^{2+} entry evoked by 8-Br-N^1-cIDPR (Figures 8k and 8l), a contribution of TRPM2 appeared possible. To analyse this in more detail, TRPM2 overexpressing HEK-293 cells were challenged with 8-Br-N^1-cIDPR; however, no significant differences to control cells were observed, although H_2O_2 (positive control) evoked huge and robust TRPM2 activation. Furthermore, the direct analysis of TRPM2 currents in patch-clamp experiments did not reveal any evidence for activation of TRPM2 by 8-Br-N^1-cIDPR. Hence, the previously published activation of TRPM2 by cADPR [28,35] appears to be due to ADPR contamination, which is present in almost all commercially available cADPR preparations (in fact they contain up to 20% of ADPR). The preparation of cADPR used in the experiments in the present study was further purified to a purity of 96%; however, higher purities are very difficult to achieve due to the instability of cADPR in solution and during freeze–thaw cycles. In contrast, a small effect attributable to cADPR was observed when it was co-infused with a low concentration of ADPR. Replacement of cADPR by 8-Br-N^1-cIDPR in such co-infusion experiments did not evoke TRPM2 currents, suggesting that the co-activating effect of cADPR on TRPM2 cannot be mimicked by 8-Br-N^1-cIDPR.

Activation of Orai1/CRACM1 channels (though not discovered at that time and thus termed capacitative Ca^{2+} entry channels) by cADPR via RyR-mediated store depletion was described for DT40B lymphoma cells lacking expression of all three subtypes of IP_3 receptors [34]. As we did not find evidence for involvement of TRPM2, activation of capacitative Ca^{2+} entry secondary to cADPR- or 8-Br-N^1-cIDPR-mediated store depletion appears the most probable process involved. This conclusion is further supported by knockdown of type 3 RyR in T-cells, resulting in significantly diminished sustained Ca^{2+} signalling [44]. Furthermore, the sensitivity of 8-Br-N^1-cIDPR-mediated Ca^{2+} entry to SKF-96365 is also in accordance with activation of capacitative Ca^{2+} entry by 8-Br-N^1-cIDPR. Interestingly, complete inhibition of Ca^{2+} entry was observed upon 8-Br-cADPR preincubation, whereas Ca^{2+} release was only partially inhibited. This obvious contradiction may be explained by the non-linear activation of capacitative Ca^{2+} entry by increasing store depletion [45]. Though this effect was explained partially by metabolism of IP_3 [45], it is not unlikely that the extent of store depletion is also not linearly coupled to activation of capacitative Ca^{2+} entry.

Taken together, we provide a detailed analysis of the mode of action of the synthetically, easily accessible and membrane-permeant cADPR agonist 8-Br-N^1-cIDPR. As 8-Br-N^1-cIDPR did not activate TRPM2, this cADPR analogue appears to be the first agonist with selectivity towards the targets RyR and TRPM2.

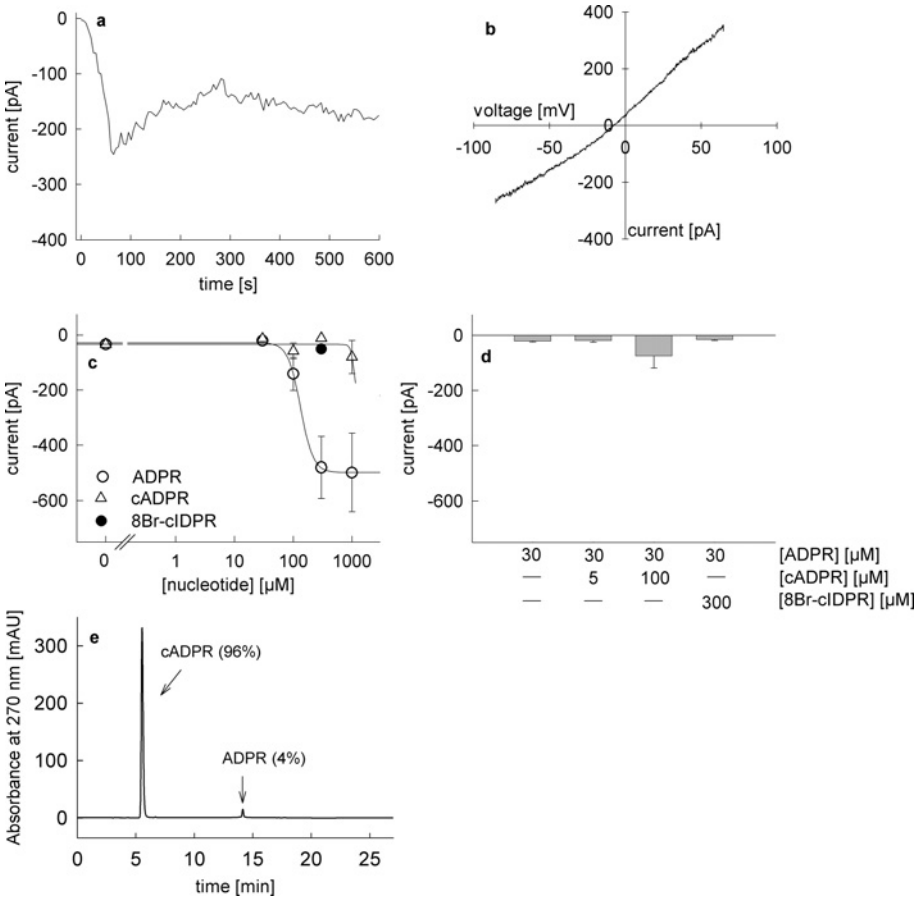

Figure 10 Activation of endogenous TRPM2 currents in Jurkat T-cells by infusion of ADPR, cADPR and 8-Br-*N*^{1}-cIDPR

All experiments were carried out with 2 mM extracellular Ca^{2+} and with unbuffered intracellular Ca^{2+} as described in [35]. Voltage ramps from -85 mV to $+65$ mV were applied every 5 s. (**a**) Representative membrane current over time recorded at -80 mV induced by perfusion with 300 μM ADPR. (**b**) Representative current–voltage relationship derived from currents evoked by voltage ramps from -85 mV to $+65$ mV. (**c**) Concentration–response relationship for activation of TRPM2 currents by infusion of ADPR (○, $n=6$–8), cADPR (△, $n=5$–8) and 300 μM 8-Br-*N*^{1}-cIDPR (●, $n=6$). Results represent means $\pm$ S.E.M. of maximum current at -80 mV. (**d**) TRPM2 currents at -80 mV after infusion of 30 μM ADPR ($n=8$), co-infusion of 5 μM cADPR and 30 μM ADPR ($n=9$), 100 μM cADPR and 30 μM ADPR ($n=8$), and 300 μM 8-Br-*N1*-cIDPR and 30 μM ADPR ($n=6$). Results represent means $\pm$ S.E.M of maximum current at -80 mV. (**e**) RP-HPLC analysis of cADPR used in the infusion experiments.

AUTHOR CONTRIBUTION

Tanja Kirchberger performed ratiometric imaging and microinjection. Tanja Kirchberger and Cornelia Siebrands carried out patch clamp experiments. Preparation and purification of 8-Br-*N*^{1}-cIDPR was performed by Christelle Moreau, Gerd Wagner and Tanja Kirchberger. Merle Nebel, Frederike Schmid and Francesca Odoardi prepared and cultured rat MBP-specific T-cells. Ralf Fliegert and Angelika Harneit developed TRPM2-expressing HEK-293 cells. Alexander Flügel, Andreas Guse and Barry Potter designed research. Tanja Kirchberger and Andreas Guse wrote the manuscript.

FUNDING

This work was supported by the Deutsche Forschungsgemeinschaft [grant numbers GU 360/9-1, GU 360/9–2]; the Gemeinnützige Hertie-Stiftung [grant number 1.01.1/07/005]; the Wellcome Trust [project grants 55709, 084068]; a Wellcome Trust Value in People award; and by a Wellcome Trust Biomedical Research Collaboration Grant [grant number 068065].

REFERENCES

1 De Flora, A., Zocchi, E., Guida, L., Franco, L. and Bruzzone, S. (2004) Autocrine and paracrine calcium signaling by the CD38/NAD$^+$/cyclic ADP-ribose system. Ann. N. Y. Acad. Sci. **1028**, 176–191
2 Guse, A. H. (2004) Biochemistry, biology, and pharmacology of cyclic adenosine diphosphoribose (cADPR). Curr. Med. Chem. **11**, 847–855
3 Guse, A. H. (2005) Second messenger function and the structure-activity relationship of cyclic adenosine diphosphoribose (cADPR). FEBS. J. **272**, 4590–4597
4 Lee, H. C. (2004) Multiplicity of Ca^{2+} messengers and Ca^{2+} stores: a perspective from cyclic ADP-ribose and NAADP. Curr. Mol. Med. **4**, 227–237
5 Lee, H. C. (2006) Structure and enzymatic functions of human CD38. Mol. Med. **12**, 317–323
6 Clapper, D. L., Walseth, T. F., Dargie, P. J. and Lee, H. C. (1987) Pyridine nucleotide metabolites stimulate calcium release from sea urchin egg microsomes desensitized to inositol trisphosphate. J. Biol. Chem. **262**, 9561–9568
7 Lee, H. C., Walseth, T. F., Bratt, G. T., Hayes, R. N. and Clapper, D. L. (1989) Structural determination of a cyclic metabolite of NAD$^+$ with intracellular Ca^{2+}-mobilizing activity. J. Biol. Chem. **264**, 1608–1615
8 Guse, A. H., Berg, I., da Silva, C. P., Potter, B. V. L. and Mayr, G. W. (1997) Ca^{2+} entry induced by cyclic ADP-ribose in intact T-lymphocytes. J. Biol. Chem. **272**, 8546–8550
9 Fruman, D. A., Klee, C. B., Bierer, B. E. and Burakoff, S. J. (1992) Calcineurin phosphatase activity in T lymphocytes is inhibited by FK 506 and cyclosporin A. Proc. Natl. Acad. Sci. U.S.A. **89**, 3686–3690
10 Crabtree, G. R. and Olson, E. N. (2002) NFAT signaling: choreographing the social lives of cells. Cell **109**, S67–S79
11 Liu, J., Koyano-Nakagawa, N., Amasaki, Y., Saito-Ohara, F., Ikeuchi, T., Imai, S., Takano, T., Arai, N., Yokota, T. and Arai, K. (1997) Calcineurin-dependent nuclear translocation of a murine transcription factor NFATx: molecular cloning and functional characterization. Mol. Biol. Cell **8**, 157–170
12 Putney, J. W. J. (1986) A model for receptor-regulated calcium entry. Cell Calcium **7**, 1–12
13 Putney, J. W. J. (2007) Recent breakthroughs in the molecular mechanism of capacitative calcium entry (with thoughts on how we got here). Cell Calcium **42**, 103–110

14 Vig, M., Peinelt, C., Beck, A., Koomoa, D. L., Rabah, D., Koblan-Huberson, M., Kraft, S., Turner, H., Fleig, A., Penner, R. and Kinet, J. (2006) CRACM1 is a plasma membrane protein essential for store-operated Ca^{2+} entry. Science **312**, 1220–1223

15 Feske, S., Gwack, Y., Prakriya, M., Srikanth, S., Puppel, S., Tanasa, B., Hogan, P. G., Lewis, R. S., Daly, M. and Rao, A. (2006) A mutation in Orai1 causes immune deficiency by abrogating CRAC channel function. Nature **441**, 179–185

16 Zhang, S. L., Yu, Y., Roos, J., Kozak, J. A., Deerinck, T. J., Ellisman, M. H., Stauderman, K. A. and Cahalan, M. D. (2005) STIM1 is a Ca^{2+} sensor that activates CRAC channels and migrates from the Ca^{2+} store to the plasma membrane. Nature **437**, 902–905

17 Guse, A. H., da Silva, C. P., Berg, I., Skapenko, A. L., Weber, K., Heyer, P., Hohenegger, M., Ashamu, G. A., Schulze-Koops, H., Potter, B. V. L. and Mayr, G. W. (1999) Regulation of calcium signalling in T lymphocytes by the second messenger cyclic ADP-ribose. Nature **398**, 70–73

18 Kirchberger, T., Wagner, G., Xu, J., Cordiglieri, C., Wang, P., Gasser, A., Fliegert, R., Bruhn, S., Flügel, A., Lund et al. (2006) Cellular effects and metabolic stability of N1-cyclic inosine diphosphoribose and its derivatives. Br. J. Pharmacol. **149**, 337–344

19 Guse, A. H., Roth, E. and Emmrich, F. (1993) Intracellular Ca^{2+} pools in Jurkat T-lymphocytes. Biochem. J. **291**, 447–451

20 Ben-Nun, A., Wekerle, H. and Cohen, I. R. (1981) The rapid isolation of clonable antigen-specific T lymphocyte lines capable of mediating autoimmune encephalomyelitis. Eur. J. Immunol. **11**, 195–199

21 Wagner, G. K., Black, S., Guse, A. H. and Potter, B. V. L. (2003) First enzymatic synthesis of an N1-cyclised cADPR (cyclic-ADP ribose) analogue with a hypoxanthine partial structure: discovery of a membrane permeant cADPR agonist. Chem. Commun. **7**, 1944–1945

22 Gasser, A. and Guse, A. H. (2005) Determination of intracellular concentrations of the TRPM2 agonist ADP-ribose by reversed-phase HPLC. J. Chromatogr. B. **821**, 181–187

23 Schweitzer, K., Mayr, G. W. and Guse, A. H. (2001) Assay for ADP-ribosyl cyclase by reverse-phase high-performance liquid chromatography. Anal. Biochem. **299**, 218–226

24 Kunerth, S., Mayr, G. W., Koch-Nolte, F. and Guse, A. H. (2003) Analysis of subcellular calcium signals in T-lymphocytes. Cell. Signal. **15**, 783–792

25 Bruzzone, S., Kunerth, S., Zocchi, E., De Flora, A. and Guse, A. H. (2003) Spatio-temporal propagation of Ca^{2+} signals by cyclic ADP-ribose in 3T3 cells stimulated via purinergic P2Y receptors. J. Cell. Biol. **163**, 837–845

26 Hamill, O. P., Marty, A., Neher, E., Sakmann, B. and Sigworth, F. J. (1981) Improved patch-clamp techniques for high-resolution current recording from cells and cell-free membrane patches. Pfugers Arch. Eur. J. Physiol. **391**, 85–100

27 Fliegert, R., Gasser, A. and Guse, A. H. (2007) Regulation of calcium signalling by adenine-based second messengers. Biochem. Soc. Trans. **35**, 109–114

28 Kolisek, M., Beck, A., Fleig, A. and Penner, R. (2005) Cyclic ADP-ribose and hydrogen peroxide synergize with ADP-ribose in the activation of TRPM2 channels. Mol. Cell **18**, 61–69

29 Togashi, K., Hara, Y., Tominaga, T., Higashi, T., Konishi, Y., Mori, Y. and Tominaga, M. (2006) TRPM2 activation by cyclic ADP-ribose at body temperature is involved in insulin secretion. EMBO. J. **25**, 1804–1815

30 Langhorst, M. F., Schwarzmann, N. and Guse, A. H. (2004) Ca^{2+} release via ryanodine receptors and Ca^{2+} entry: major mechanisms in NAADP-mediated Ca^{2+} signaling in T-lymphocytes. Cell. Signal. **16**, 1283–1289

31 Kerschbaum, H. H. and Cahalan, M. D. (1999) Single-channel recording of a store-operated Ca^{2+} channel in Jurkat T lymphocytes. Science **283**, 836–839

32 Herscher, C. J. and Rega, A. F. (1996) Pre-steady-state kinetic study of the mechanism of inhibition of the plasma membrane Ca(2+)-ATPase by lanthanum. Biochemistry **35**, 14917–14922

33 Zhang, B., Wagner, G. K., Weber, K., Garnham, C., Morgan, A. J., Galione, A., Guse, A. H. and Potter, B. V. L. (2008) 2′-deoxy cyclic adenosine 5′-diphosphate ribose derivatives: importance of the 2′-hydroxyl motif for the antagonistic activity of 8-substituted cADPR derivatives. J. Med. Chem. **51**, 1623–1636

34 Kiselyov, K., Shin, D. M., Shcheynikov, N., Kurosaki, T. and Muallem, S. (2001) Regulation of Ca^{2+}-release-activated Ca^{2+} current (I_{crac}) by ryanodine receptors in inositol 1,4,5-trisphosphate-receptor-deficient DT40 cells. Biochem. J. **360**, 17–22

35 Beck, A., Kolisek, M., Bagley, L. A., Fleig, A. and Penner, R. (2006) Nicotinic acid adenine dinucleotide phosphate and cyclic ADP-ribose regulate TRPM2 channels in T lymphocytes. FASEB. J. **20**, 962–964

36 Gasser, A., Bruhn, S. and Guse, A. H. (2006) Second messenger function of nicotinic acid adenine dinucleotide phosphate revealed by an improved enzymatic cycling assay. J. Biol. Chem. **281**, 16906–16913

37 Guse, A. H. and Lee, H. C. (2008) NAADP: a universal Ca^{2+} trigger. Sci. Signal. **1**, re10

38 Guse, A. H., Goldwich, A., Weber, K. and Mayr, G. W. (1995) Non-radioactive, isomer-specific inositol phosphate mass determinations: high-performance liquid chromatography-micro-metal-dye detection strongly improves speed and sensitivity of analyses from cells and micro-enzyme assays. J. Chromatogr. B. Biomed. Appl. **672**, 189–198

39 Gu, X., Yang, Z., Zhang, L., Kunerth, S., Fliegert, R., Weber, K., Guse, A. H. and Zhang, L. (2004) Synthesis and biological evaluation of novel membrane-permeant cyclic ADP-ribose mimics: *N*1-[(5′′-*O*-phosphorylethoxy)methyl]-5′-*O*-phosphorylinosine 5′,5′′-cyclicpyrophosphate (cIDPRE) and 8-substituted derivatives. J. Med. Chem. **47**, 5674–5682

40 Guse, A. H., Gu, X., Zhang, L., Weber, K., Kramer, E., Yang, Z., Jin, H., Li, Q., Carrier, L. and Zhang, L. (2005) A minimal structural analogue of cyclic ADP-ribose: synthesis and calcium release activity in mammalian cells. J. Biol. Chem. **280**, 15952–15959

41 Kudoh, T., Fukuoka, M., Ichikawa, S., Murayama, T., Ogawa, Y., Hashii, M., Higashida, H., Kunerth, S., Weber, K., Guse, A. H., et al. (2005) Synthesis of stable and cell-type selective analogues of cyclic ADP-ribose, a Ca^{2+}-mobilizing second messenger. Structure–activity relationship of the N1-ribose moiety. J. Am. Chem. Soc. **127**, 8846–8855

42 Moreau, C., Wagner, G. K., Weber, K., Guse, A. H. and Potter, B. V. L. (2006) Structural determinants for N1/N7 cyclization of nicotinamide hypoxanthine 5′-dinucleotide (NHD^+) derivatives by ADP-ribosyl cyclase from *Aplysia californica*: Ca^{2+}-mobilizing activity of 8-substituted cyclic inosine 5′-diphosphoribose analogues in T-lymphocytes. J. Med. Chem. **49**, 5162–5176

43 Xu, J., Yang, Z., Dammermann, W., Zhang, L., Guse, A. H. and Zhang, L. (2006) Synthesis and agonist activity of cyclic ADP-ribose analogues with substitution of the northern ribose by ether or alkane chains. J. Med. Chem. **49**, 5501–5512

44 Schwarzmann, N., Kunerth, S., Weber, K., Mayr, G. W. and Guse, A. H. (2002) Knock-down of the type 3 ryanodine receptor impairs sustained Ca^{2+} signaling via the T cell receptor/CD3 complex. J. Biol. Chem. **277**, 50636–50642

45 Parekh, A. B., Fleig, A. and Penner, R. (1997) The store-operated calcium current I_{CRAC}: nonlinear activation by $InsP_3$ and dissociation from calcium release. Cell **89**, 973–980

Received 28 November 2008/29 May 2009; accepted 3 June 2009
Published as BJ Immediate Publication 3 June 2009, doi:10.1042/BJ20082308